Research Article

Design, Manufacturing, and Characterization of High-Performance Lightweight Bipolar Plates Based on Carbon Nanotube-Exfoliated Graphite Nanoplatelet Hybrid Nanocomposites

Myungsoo Kim,[1] Gu-Hyeok Kang,[1] Hyung Wook Park,[1] Young-Bin Park,[1] Yeon Ho Park,[2] and Kwan Han Yoon[2]

[1] *School of Mechanical and Advanced Materials Engineering, Ulsan National Institute of Science and Technology, UNIST-gil 50, Eonyang-eup, Ulju-gun, Ulsan 689-798, Republic of Korea*
[2] *Department of Polymer Science and Engineering, Kumoh National Institute of Technology, 1 Yangho-dong, Gumi, Gyeongbuk 730-701, Republic of Korea*

Correspondence should be addressed to Young-Bin Park, ypark@unist.ac.kr and Kwan Han Yoon, khyoon@kumoh.ac.kr

We report a study on manufacturing and characterization of a platform material for high-performance lightweight bipolar plates for fuel cells based on nanocomposites consisting of carbon nanotubes (CNTs) and exfoliated graphite nanoplatelets (xGnPs). The experiments were designed and performed in three steps. In the preexperimental stage, xGnP-epoxy composite samples were prepared at various xGnP weight percentages to determine the maximum processable nanofiller concentration. The main part of the experiment employed the statistics-based design of experiments (DOE) methodology to identify improved processing conditions and CNT : xGnP ratio for minimized electrical resistivity. In the postexperimental stage, optimized combinations of material and processing parameters were investigated. With the aid of a reactive diluent, 20 wt.% was determined to the be maximum processable carbon nanomaterial content in the epoxy. The DOE analyses revealed that the CNT : xGnP ratio is the most dominant factor that governs the electrical properties, and its implications in relation to CNT-xGnP interactions and microstructure are elucidated. In addition, samples fabricated near the optimized condition revealed that there exists an optimal CNT : xGnP ratio at which the electrical performance can be maximized. The electrical and mechanical properties of optimal samples suggest that CNT-xGnP hybrid nanocomposites can serve as an alternative material platform for affordable, lightweight bipolar plates.

1. Introduction

The increase of global population and rapid development of various industrial sectors, including manufacturing and transportation, have dramatically increased fossil energy consumption. With growing concerns on petroleum depletion, many countries have been trying to identify alternative energy sources that can replace fossil energy. In this regard, fuel cells have been drawing increasing attention, and the demand for developing high-performance fuel cells has grown recently [1–3]. Fuel cells can be categorized into six groups: (i) proton exchange membrane fuel cell (PEMFC), including direct methanol fuel cell (DMFC), (ii) alkaline fuel cell (AFC), (iii) phosphoric acid fuel cell (PAFC), (iv) molten carbonate fuel cell (MCFC), (v) solid oxide fuel cell (SOFC), and (vi) microbial fuel cell (MFC). Currently, PEMFC is a promising power source for various application fields owing to its attractive features, such as wide range of working temperature and high power density [4–6].

PEMFC consists of four major parts: proton exchange membrane, catalyst layer, diffusion layer, and bipolar plate. Bipolar plates account for 60–80% of weight and 29–45%

of cost of fuel cell stacks [3]. Hence, employing lightweight materials for bipolar plates is critical for reducing the weight and cost of fuel cells [7]. Bipolar plates have a number of functions within a fuel cell stack. They connect cells electrically in series, separate the gases in adjacent cells, provide solid structure for the stack, transfer heat out of the cell, and typically house the flow field channels. To meet these performance requirements, bipolar plates should have several characteristics including high electrical conductivity, good mechanical properties, high thermal conductivity, impermeability to gasses, low cost, light weight, good processability, and resistance to corrosion [3, 8].

Graphite and metal are commonly used to fabricate bipolar plates. Graphite is marked by high electrical conductivity and corrosion resistance, but it has several disadvantages, such as brittleness, low workability, and high cost. Metal alloys also have advantages and disadvantages as the materials for bipolar plates. They are characterized by high mechanical strength, flexibility, and electrical and thermal conductivities. However, their applications are hindered by low corrosion resistance in the high-acidity, high-humidity operating environment of fuel cells [3]. Metal- or graphite-reinforced composites are also used to meet the requirement for bipolar plate. However, the performance requirements demand 50–70% filler volume content, which would dramatically increase the cost and adversely affect processing. High filler concentration tends to generate internal defects, high wear rate of mold, and high viscosity during processing. Moreover, it renders the bipolar plate brittle and permeable because of low relative polymer matrix content [9, 10]. To overcome these shortcomings, carbon nanomaterials, such as carbon black, carbon nanotube (CNT) exfoliated graphite nanoplatelet (xGnP), have been considered as candidate fillers, as they are marked by excellent electrical and mechanical properties with large surface areas and high aspect ratios, which would allow significant reduction of filler content [11, 12].

In this paper, CNT-xGnP-hybridized epoxy nanocomposites are explored as the materials for high-performance, lightweight bipolar plates. To improve the electrical conductivity, which is one of the most critical factors for bipolar plates, CNT : xGnP ratio and nanocomposite manufacturing process parameters were investigated using the statistics-based design of experiments (DOE) methodology. The influential material and process parameters were identified, and the optimal processing conditions were found, based on which nanocomposite samples were fabricated and characterized. Electrical and mechanical properties were measured, and SEM images were analyzed to validate the experimental results.

2. Experimental

2.1. Materials.
CVD-grown multiwalled carbon nanotubes (MWCNTs, CM-250) were supplied by Hanwha Nanotech (Incheon, Korea). The diameter of the CNTs was 10–15 nm, and the average length was 100 μm. The xGnPs (M-15) used in this research were provided by XG Sciences (Lansing, MI, USA). The lateral dimension and thickness

of xGnP were ~15 μm and 5–15 nm, respectively. xGnP is composed of tens of layers of graphene nanosheets, and the electrical conductivity, as provided by the manufacturer, is 10^7 S/m in in-plane and 10^2 S/m in through-thickness directions. Accordingly, the average electrical conductivity of xGnPs randomly oriented in a polymer would be between 10^2 S/m and 10^7 S/m. The in-plane tensile modulus of xGnP is 1000 GPa. The bisphenol-F epoxy resin (YDF-170) and curing agent (SH-101) were supplied by Kukdo Chemical (Seoul, Korea) and Sejin E&C (Yangsan, Korea), respectively. To reduce the viscosity of carbon nanomaterial-epoxy resin mixture, an aliphatic-glycidyl-ether-based reactive diluent (BGE) supplied by Kukdo Chemical (Seoul, Korea) was used. The manufacturer-recommended composition of the 100 : 25 ratio between resin and curing agent by weight was used, and the amount of reactive diluents was 10% by weight with respect to the resin.

2.2. Experiment Design.
Three sets of experiment were performed. The first set aimed at determining the maximum xGnP concentration in an xGnP-epoxy nanocomposite from the processing standpoint. The second set employed the design of experiments (DOE) techniques [13] to design the experiments, identify influential parameters, study parameter interactions, if any, and determine the optimal material and process parameter combinations for minimized electrical resistivity. In the third set of experiment, the optimized conditions found in the second set were used to fabricate CNT-xGnP epoxy composites for validation purposes.

Table 1 shows the control factors (or parameters) and their low and high levels used in the second set of experiment. In the table, CNT : xGnP represents the weight ratio between CNT and xGnP. The other two factors are associated with the equipment used to disperse the carbon nanomaterials in the epoxy resin, known as three-roll mill. As shown in Figure 1, the three-roll mill consists of three rollers between which the resin mixture passes through as the rollers rotate in the directions shown. The equipment is set up such that the rotational speeds of the rollers are in a ratio of 1 : 3 : 9. The different rotational speeds generate shear in the resin mixture, which allows exfoliation and uniform distribution of carbon nanomaterial aggregates. The two processing-related factors are "No. Pass," which is the number the carbon nanomaterial-epoxy mixture passes through the rollers and "Roller rpm," which is the rotational speed of Roller 3. The gaps between the rollers were fixed at 5 μm. The response, which is the physically meaningful output of the experiment, is volume resistivity ($\Omega \cdot$cm). The objective of DOE was to determine the optimal combinations of the control factors that minimize the volume resistivity.

2.3. The Manufacturing Process.
In the first set of experiment, 1, 5, 10, 15, 25, and 30 wt.% xGnP-epoxy composites were fabricated. Weighed amounts of xGnP and epoxy were premixed using a paste mixer (PDM-300) manufactured by Dae Wha Tech (Yongin, Korea) and were subsequently calendered using a three-roll mill (80S, silicon carbide rolls) manufactured by EXAKT (Germany). The rotational speed

TABLE 1: Control factors and levels.

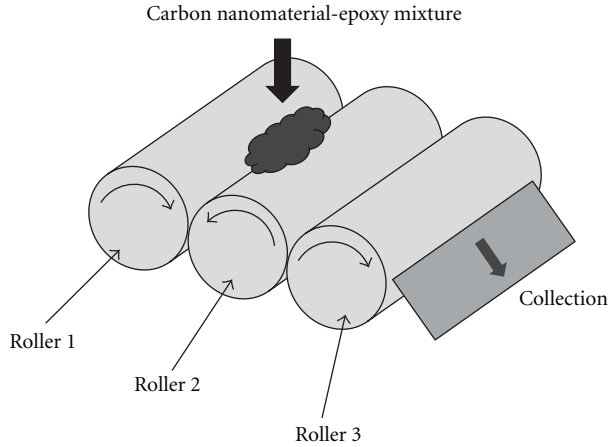| Factor	Coded symbol	Low (−1)	High (1)	Middle (0)
CNT : xGnP (weight ratio)	A	20 / 20 (CNT) : 80 (xGnP)	80 / 80 (CNT) : 20 (xGnP)	50 / 50 (CNT) : 50 (xGnP)
Roller rpm	B	90	180	135
No. Pass	C	10	20	15

FIGURE 1: Schematic of three-roll mill.

of Roller 3 was 256 rpm. After being passed through the three-roll mill 20 times, a curing agent was added, and the mixture was stirred and degassed under vacuum for 30 min. The mixture was poured into an aluminum mold, which was placed in a heated press (Carver 4386, Wabash, IN, USA). The nanocomposite mixture was cured at 120°C for 2 hr and postcured at 150°C for 2 hr, resulting in a 100 mm by 100 mm nanocomposite sheet with a thickness of 2 mm.

In the second set of experiment, a fixed carbon nanomaterial content of 20 wt.% was used to fabricate and characterize the nanocomposite samples. The total weight percent of CNT and xGnP combined was 20, and the CNT : xGnP ratio by weight varied from 80 : 20 to 50 : 50 and 20 : 80. In the third set of experiment, the CNT : xGnP ratios of 100 : 0 and 90 : 10 were used to experimentally validate the optimal material and process parameters determined by DOE. The same nano-filler dispersion and nanocomposite sheet fabrication methods as the first set of experiment were employed.

2.4. Characterization. The volume resistivities of high-resistivity nanocomposite samples were measured per ASTM (American Society for Testing and Materials) D257 using a resistance test fixture (model 8009) and high-resistance digital multimeter (model 6517B, ±1% measurement accuracy), manufactured by Keithley (Cleveland, OH, USA). Low-resistivity samples were measured using a four-point probe surface resistance measurement system (CMT-SR1000N, ±0.5% measurement accuracy) manufactured by Advanced Instrument Technology (Suwon, Korea). The surface resistance measurement system provides volume resistivity based

on the measured surface resistance and thickness of the sample. The surface resistivities were measured on both sides and averaged. The nanocomposite sheets were cut using a 40-watt laser cutter (Industrial Series) manufactured by Universal Laser Systems (Scottsdale, AZ, USA), and tensile and flexural properties were measured in accordance with ASTM D638 and D790, respectively, using a universal material testing system (model 5982) equipped with a 100-kN load cell, manufactured by Instron (Norwood, MA, USA). The microstructure of the fracture surfaces of selected nanocomposites was observed and analyzed using a scanning electron microscope (SEM, Nanonova 230), manufactured by FEI (Hillsboro, OR, USA).

3. Results and Discussion

3.1. Determination of Maximum xGnP Loading (Experiment 1). In the first set of experiment, xGnP-epoxy composite samples with 1, 5, 10, 15, 25, and 30 wt.% xGnP loadings were prepared and tested to determine the maximum processablexGnP content. Nanocomposites with xGnP loadings higher than 20 wt.% could not be prepared due to various processing issues. At 30 wt.%, the premixed xGnP-epoxy mixture after being treated with a paste mixer behaved as a solid (much like powder), which did not allow subsequent processing in a three-roll mill. At 25 wt.%, the xGnP-epoxy composite sheet strongly adhered to the mold surface, even with the use of a mold releasing agent, which may be due to the high pressure generated thermal expansion of the mold. Therefore, the maximum xGnP loading was determined to be 20 wt.%.

The measured resistivities of the nanocomposite samples are shown in Table 2. A high-resistance digital multimeter and a four-point probe resistivity measurement system were used to measure volume resistivities of high-resistivity samples (0, 1, 5 wt.%) and low-resistivity samples (10, 15, 25 wt.%), respectively. It seems that the xGnP-epoxy composites with 0–10 wt.% xGnP are not suitable for bipolar plates because of high resistivities. The electrical conductivity plot, converted from the resistivities, show a class "S-curve" as a function of filler volume fraction, characterized by a percolation threshold between 2.8 and 6.2 vol.% (equivalent to 4.6 and 10 wt.%), at which a dramatic transition from insulation to conduction is observed (Figure 2). The volume percent in Table 2 was calculated using the following equation [14]:

$$V_{xGnP} = \frac{W_{xGnP}}{W_{xGnP} + (\rho_{xGnP}/\rho_m) - (\rho_{xGnP}/\rho_m) W_{xGnP}}, \quad (1)$$

TABLE 2: Electrical properties of nanocomposites from Experiment 1.

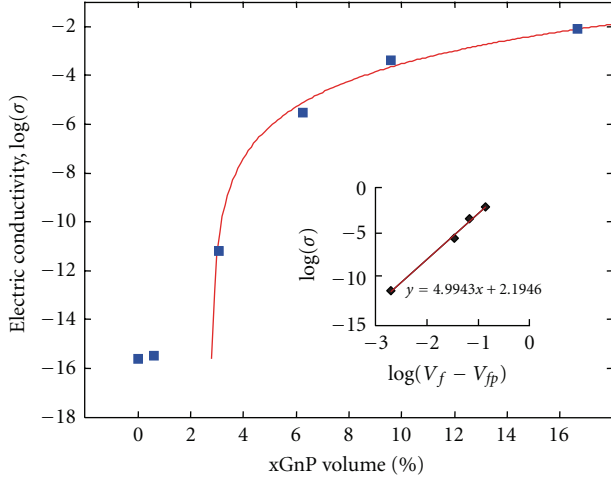| wt.%	vol.%	Volume resistivity ($\Omega\cdot$cm)	Volume conductivity σ (S/cm)	Log(σ)
0	0	$4.03 \times 10^{15} \pm 8.39 \times 10^{14}$	$2.58 \times 10^{-16} \pm 6.05 \times 10^{-17}$	-15.60 ± 0.10
1	0.6	$3.07 \times 10^{15} \pm 7.24 \times 10^{14}$	$3.42 \times 10^{-16} \pm 8.38 \times 10^{-17}$	-15.48 ± 0.11
5	3.0	$1.95 \times 10^{11} \pm 1.14 \times 10^{11}$	$7.73 \times 10^{-12} \pm 6.12 \times 10^{-12}$	-11.21 ± 0.31
10	6.2	$3.35 \times 10^{5} \pm 8.65 \times 10^{4}$	$3.16 \times 10^{-6} \pm 7.86 \times 10^{-7}$	-5.51 ± 0.11
15	9.5	$2.55 \times 10^{3} \pm 8.72 \times 10^{2}$	$4.31 \times 10^{-4} \pm 1.40 \times 10^{-4}$	-3.39 ± 0.15
25	16.5	$1.26 \times 10^{2} \pm 1.11 \times 10^{1}$	$8.01 \times 10^{-3} \pm 7.23 \times 10^{-4}$	-2.10 ± 0.04

FIGURE 2: Measured and predicted electrical conductivities of xGnP-epoxy composites.

where ρ_{xGnP} and ρ_m represent the densities of xGnP (2.0 g/cm^3) and epoxy (1.2 g/cm^3), respectively [15]. W_{xGnP} denotes the weight fractions of xGnP in the matrix. The conductivity of the 25 wt.% xGnP sample, which was the sample with the highest xGnP loading of which the resistivity could be measured, showed as much as thirteen orders of magnitude higher conductivity as compared to neat epoxy.

The electrical property data were analyzed in conjunction with the percolation theory, which correlates filler content and electrical conductivity. The relationship is given by the following power-law equation [16–20]:

$$\sigma = \sigma_f \left(V_f - V_{fp} \right)^t, \qquad (2)$$

where σ is the electrical conductivity of composite, σ_f is the adjustable parameter, V_f is the filler volume fraction, V_{fp} is the critical filler volume fraction at the percolation threshold, and t is the critical exponent. This theory gives a good description of experimental results near the transition point, and the power-law relationship is valid only above the percolation threshold, that is, when $V_f > V_{fp}$. The values of the parameter σ_f, the percolation threshold concentration V_{fp}, and the critical exponent t were determined using the least squares fit, as shown in Figure 2 using (3) [21].

The inset in Figure 2, which presents the log(σ) versus log($V_f - V_{fp}$) relationship from the experimental data

from 5 to 25 wt.% in Table 2, shows a good qualitative correspondence between the experimental data and theoretical prediction. From the least squares fit, 150 S/cm, 2.8 vol.%, and 4.99 were obtained, respectively, for σ_f, V_{fp}, and the exponent t in (2). The xGnP's percolation of 2.8 vol.% (equivalent to 4.6 wt.%) is also slightly higher than typical percolation thresholds of CNT polymer composites (<3 wt.%) [22–25], the reason for which is explained in Section 3.2. Typical t values are in the range of 1.6–1.9 for three-dimensional systems [16–20]; however, a number of researchers have reported that the critical exponent could be as high as 2, 3, or even much higher [18–20, 26, 27] because of special geometry, tunneling effect, and coalescence of conducting particles [28]. With the obtained coefficients, the percolation theory in (2) fits the experimental data fairly well.

3.2. Parametric Study Using DOE (Experiment 2). In this section, the processing-structure-property relationship of CNT-xGnP-epoxy hybrid nanocomposites is discussed. Table 3 shows the DOE-generated combinations of CNT : xGnP ratio, manufacturing process parameters (roller rpm and number of passes through the three-roll mill), and average resistivities measured. A full-factorial design with three factors was used, and ten experimental combinations at eight factorial (corner) points ($2^3 = 8$) and two center points were performed. The experimental data were analyzed using the Design Expert software, commercially available from Stat-Ease.

Based on the half normal plot in Figure 3, the model includes the factors, A, C, AC, B, and AB. Here, AC and AB represent the interactions between the respective two factors. The farther away the factors are located from the solid line, the more influential the factors are. Therefore, factor A, the weight ratio between CNT and xGnP, is the most significant factor in the model. The analysis of variance confirmed that the model was significant, and therefore, the selected factors highly affect the results.

The regression model for resistivity in terms of coded factors can be expressed as

$$\text{Resistivity} = +0.81 - 0.36 * A - 0.11 * B + 0.20 * C$$
$$+ 0.09 * A * B - 0.15 * A * C. \qquad (3)$$

TABLE 3: DOE-generated control factors and experimental results.

Run	CNT : xGnP (weight ratio), (A)	Roller rpm (B)	No. Pass (C)	Resistivity ($\Omega \cdot$cm)
1	80 : 20	90	20	0.565 ± 0.043
2	50 : 50	135	15	0.528 ± 0.059
3	80 : 20	180	10	0.413 ± 0.019
4	20 : 80	90	20	1.835 ± 0.105
5	80 : 20	90	10	0.409 ± 0.0114
6	20 : 80	180	10	0.695 ± 0.033
7	80 : 20	180	20	0.469 ± 0.036
8	20 : 80	180	20	1.261 ± 0.048
9	50 : 50	135	15	0.462 ± 0.053
10	20 : 80	90	10	1.021 ± 0.095

Design-expert plot resistivity
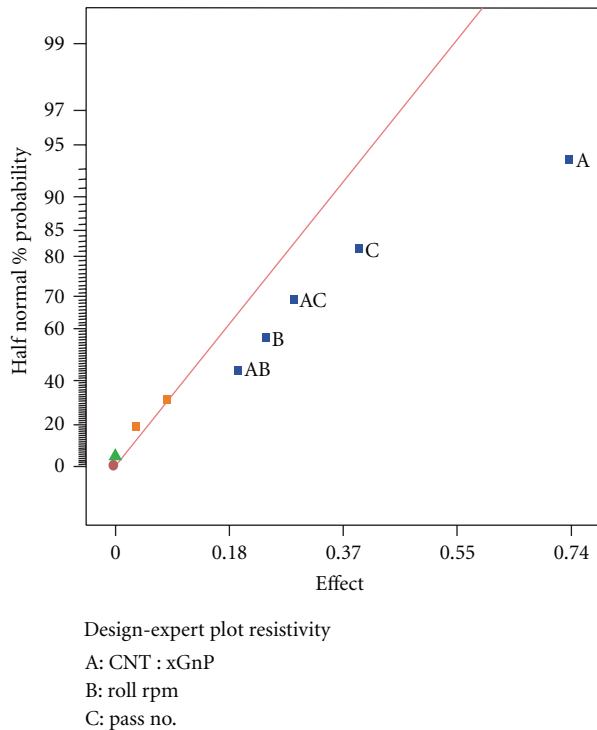
A: CNT : xGnP
B: roll rpm
C: pass no.

FIGURE 3: Half normal plot.

The regression model for resistivity in terms of actual factors can be expressed as

$$
\begin{aligned}
\text{Resistivity} = {} & 0.86988 - 6.03535E - 003 * \text{CNT ratio} \\
& - 5.88677E - 003 * \text{roller rpm} \\
& + 0.089338 * \text{No. pass} + 6.66489E - 005 \\
& * \text{CNT ratio} * \text{roller rpm} \\
& - 9.98057E - 004 * \text{CNT ratio} * \text{No. pass}.
\end{aligned}
\tag{4}
$$

The coded factors used the coded values ($-1 \leq$ A, B, C $\leq$ 1), while the actuarial factors used the real values (e.g., 20 $\leq$ CNT % ratio $\leq$ 80 for CNT weight ratio (see Table 1)).

As for factor A (the weight ratio between CNT and xGnPs), the average resistivity results with lower level (Runs 4, 6, 8, and 10 in Table 3) and higher level (Runs 1, 3, 5, and 7) were 1.203 $\Omega \cdot$cm and 0.464 $\Omega \cdot$cm, respectively. In other words, as the xGnP content decreases and the CNT content increases, the volume resistivity decreases, that is, the nanocomposite becomes more conductive. As mentioned in Section 2.1, the resistivity of xGnP in the through-thickness direction is higher than the in-plane resistivity, which is close to the resistivity of CNT. Hence, if xGnPs are in random orientation, it is likely that the general volume resistivity of xGnP is higher than that of CNT. Therefore, as the CNT : xGnP ratio increases, the volume resistivity of composite decreases. Another factor that needs to be taken into account is the interfacial bonding between xGnP and epoxy matrix, as evidenced by the SEM image of the fracture surface of a CNT-xGnP-epoxy composite in Figure 4. Poor interfacial bonding interferes with electron transport—both ballistic and tunneling (or electron hopping)—within the composite, resulting in an increase in resistivity. This might be the reason why xGnP's percolation threshold was slightly higher than CNT's percolation as mentioned in Section 3.1.

The average resistivity of Runs 2 and 9 (middle points) from Table 3 was 0.495 $\Omega \cdot$cm which is close to the higher level resistivity of Factor A, 0.464 $\Omega \cdot$cm, and not near the average of higher and lower level resistivities of Factor A, that is, 0.83 $\Omega \cdot$cm (= (1.203+0.464)/2). This implies that the curvature is significant, and it is recommended that the resistivity around the center point should be investigated.

As for Factor B (the rotational speed of Roller 3 in the three-roll mill), the average resistivity results from lower level (Runs 1, 4, 5, and 10) and higher level (Runs 3, 6, 7, and 8) were 0.9575 and 0.7095 $\Omega \cdot$cm, respectively. The general trend is that resistivity decreases as the roller speed increases. A higher roller speed means a larger relative speed difference among the three rollers; hence larger shear stresses, similar to the flow between plates, resulting in more uniform dispersion of carbon nanomaterials in the resin.
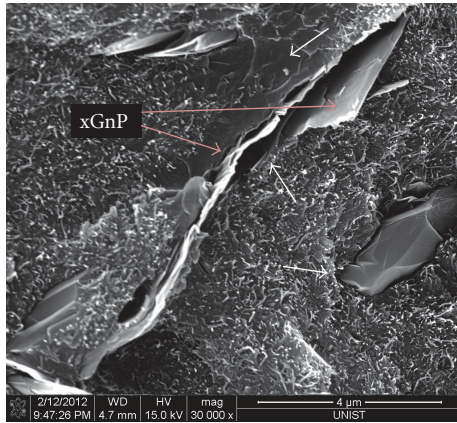
FIGURE 4: SEM image of Run 3 sample.

TABLE 4: Selected manufacturing processes for optimization.

CNT (%) : xGnP (%)	Roller angular speed (rpm)	No. of passes
100 : 0	130	40
90 : 10	130	20

Judging from the average resistivity in regard to Factor C (0.6345 $\Omega \cdot$ cm for 10 passes and 1.0325 $\Omega \cdot$ cm for 20 passes), a higher number of passes resulted in higher resistivity. This may be due to the fact that subjecting the carbon nanomaterial-resin mixture to repetitive high-shear environment results in shortening of CNTs and even in breaking of xGnPs into smaller particles, which would lead to less efficient formation of conductive network in the resin. The damages incurred on the nanomaterials are likely to depend on roller gaps and warrant further investigation.

3.3. Material and Process Optimization (Experiment 3). To minimize the volume resistivity, numerical optimization was performed with the regression models, (3) and (4), using Design Expert. The search areas (or ranges) were 0–100% for CNT concentration in 20 wt.% nanofiller, 50–250 rpm for roller speed, and 5–40 passes. Design Expert recommended a list of optimal fabrication process parameters, among which two parameter combinations as shown in Table 4 were selected for further studies.

The measured resistivities of 100% (CNT) : 0% (xGnP) and 90% (CNT) : 10% (xGnP) samples were 0.540±0.016 and 0.507±0.023 $\Omega \cdot$ cm, respectively, which are only slightly higher than the average resistivity of 80% (CNT) : 20% (xGnP) samples, 0.464 $\Omega \cdot$ cm. Since the volume resistivity decreases as CNT content increases as mentioned in Section 3.2, the resistivity of 90% and 100%-CNT samples was expected to have lower values than that of 80%-CNT samples. This phenomenon could be explained with the schematic illustrated in Figure 5, which is derive from the discrepancies in the nature of one-dimensional (CNT) and two-dimensional (xGnP) nanoparticles. Since xGnP is capable of covering larger, micron-scale areas than CNT, the
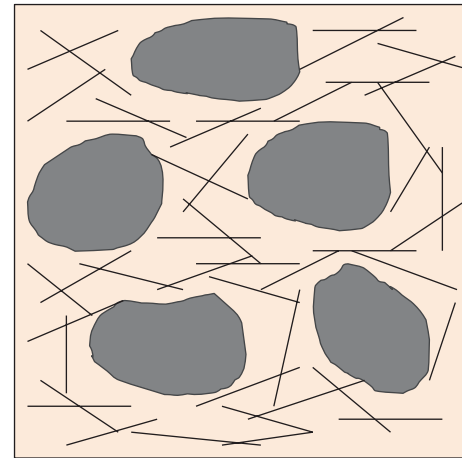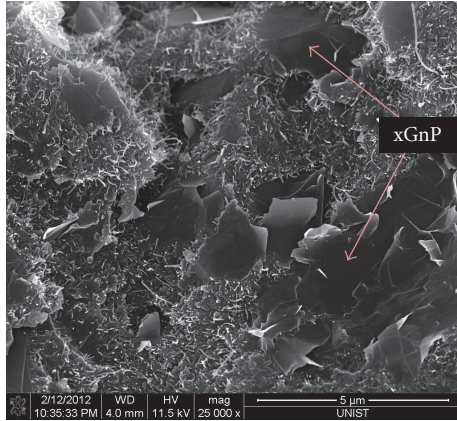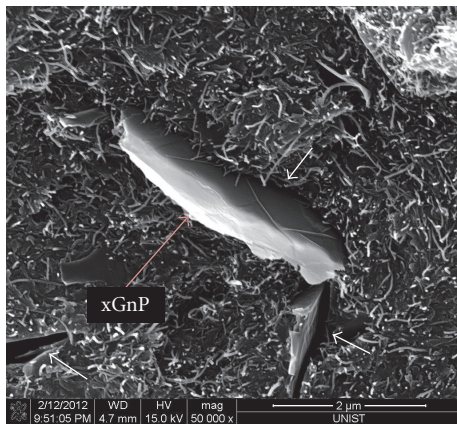

(a)
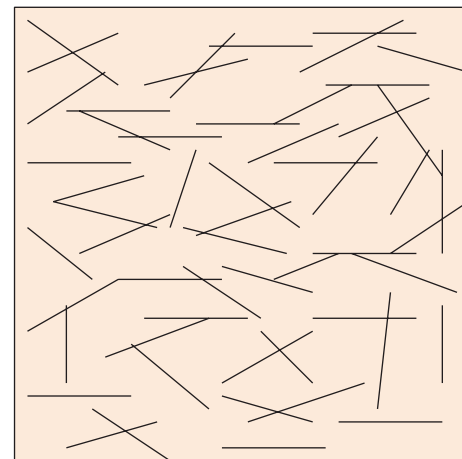
(b)

FIGURE 5: Schematic of two-dimensional xGnPs and rod-shaped CNTs in epoxy: (a) 80% (CNT) : 20% (xGnP) and (b) 100% (CNT) : 0% (xGnP).

absence of xGnPs results in the reduction of conducting-material-rich area in the epoxy matrix. On the other hand, if only xGnPs form a conductive network, the interparticle distance increases, as the overall surface area of the fillers decreases, resulting in an increase in resistivity. Therefore, there exists an optimal CNT : xGnP ratio (e.g., 80 : 20 in our case), at which the balance between the areal coverage by xGnPs and the bridging effect of CNTs among the xGnPs is optimized. Figure 6 shows the SEM images of Run 5 sample (80%-CNT and 20%-xGnP) whose schematic is shown in Figure 5(a).

3.4. Mechanical Property Characterization. Mechanical tests were performed to characterize the flexural and tensile properties of selected nanocomposite samples. Since fuel cell bipolar plates require low volume resistivity, specimens from Runs 3 and 5 in Table 3, which showed the lowest resistivities of 0.413 and 0.409 $\Omega \cdot$ cm, respectively, among all the runs, were chosen.

(a) low magnification (25,000X)

(b) high magnification (50,000X)

FIGURE 6: SEM images of Run 5 sample, 80% (CNT) : 20% (xGnP).

TABLE 5: Average flexural properties of samples from Runs 3 and 5.

Flexural modulus (GPa)	Maximum stress (MPa)	Maximum strain (%)
5.72 ± 0.08	89.4 ± 6.5	1.6 ± 0.1

TABLE 6: Average tensile properties of samples from Runs 3 and 5.

Tensile modulus (GPa)	Ultimate tensile strength (MPa)	Maximum strain (%)
2.14 ± 0.27	53.1 ± 13.8	4.5 ± 1.3

4. Conclusions

Hybrid epoxy composites filled with CNTs and xGnPs have been fabricated and characterized to investigate their potential application as the platform material for high-performance, lightweight bipolar plates for fuel cells. From the first set of experiment, it was concluded that 20 weight percent of xGnP was the maximum xGnP loading in an epoxy matrix from the processing standpoint. The electrical conductivities of xGnP-epoxy composites exhibited a classic "S-curve" as a function of xGnP volume fraction, and the trend showed a good agreement with the values predicted from the percolation-theory-based power-law relationship. In the second set of experiment, epoxy composite containing 20 weight percent of carbon nanomaterials at various CNT : xGnP ratios (80 : 20, 50 : 50, 20 : 80) were investigated. The statistics-based DOE techniques were utilized to identify dominant material and process parameters and to study factor effects and interactions. The CNT : xGnP ratio was determined to be the most influential parameter, as compared to the rotational speed of roller and the number of passes through the three-roll mill. In addition, the interactions between factors were insignificant. In the third set of experiment, DOE was further applied to determine optimal parameter combinations that minimize the resistivity. It was revealed that there exists an optimal CNT : xGnP ratio (80 : 20 in our research) that minimizes the resistivity, which is attributed to the effects of interactions between one-dimensional CNTs and two-dimensional xGnPs on the efficiency of conductive network formation. From the flexural tests, the average flexural strength of the best-case samples was measured to be 89.38 MPa, which meets the year 2015 technical target proposed by the US DoE, 25 MPa. In summary, CNT-xGnP hybrid epoxy composites serve as a potential material platform for fuel cell bipolar plate application that can meet the electrical and mechanical requirements imposed by the US DoE. It would be possible for them to substitute conventional metal- or graphite-based bipolar plates by improving weight, performance, and durability, while maintaining affordability.
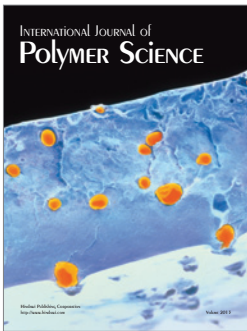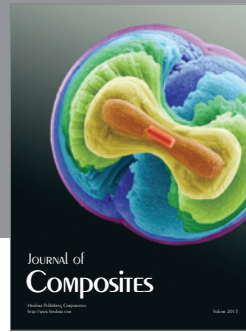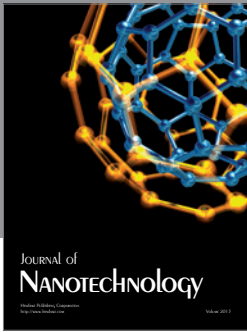
Acknowledgment

Flexural test specimens were rectangular-shaped specimens measuring 55 mm (L) 12 mm (W) by with a thickness (T) of 2 mm. Span of 32 mm and crosshead speed of 1 mm/min were employed. The flexural properties summarized in Table 5 show an average flexural strength of 89.4 MPa, which far exceeds the year 2015 technical target of 25 MPa proposed by the US Department of Energy (DoE) for fuel cell bipolar plate applications [3]. As compared to the measured flexural properties of neat epoxy (modulus = 3.7 GPa, strength = 171.9 MPa, and maximum strain = 7.6%), the average modulus of specimens from Runs 3 and 5 increased by 54%, while strength and % maximum strain decreased significantly.

Tensile tests were performed using dog-bone-shaped tensile test specimens measuring 3.4 mm (W) and 2 mm (T) in the narrow section. The tensile properties are summarized in Table 6. As compared to the tensile properties of fully-cured neat epoxy (tensile modulus = 1.61 GPa, ultimate tensile strength = 81.4 MPa, elongation = 10.2%), as measured using the control specimens, the 20 wt.% CNT-xGnP hybrid composites from Runs 3 and 5 showed an improved modulus (by 33%), while strength and % elongation to break decreased significantly, which may be attributed to poor filler-matrix bonding and the presence of reactive diluent.

References

[1] F. Panik, "Fuel cells for vehicle applications in cars—bringing the future closer," *Journal of Power Sources*, vol. 71, pp. 36–38, 1998.

[2] S. G. Kandlikar and Z. Lu, "Thermal management issues in a PEMFC stack—a brief review of current status," *Applied Thermal Engineering*, vol. 29, no. 7, pp. 1276–1280, 2009.

[3] S. C. Tjong, "Polymer nanocomposite bipolar plates reinforced with carbon nanotubes and graphite nanosheets," *Energy and Environmental Science*, vol. 4, no. 3, pp. 605–626, 2011.

[4] S. Mekhilef, R. Saidur, and A. Safari, "Comparative study of different fuel cell technologies," *Renewable and Sustainable Energy Reviews*, vol. 16, pp. 981–989, 2012.

[5] P. Tomczyk, "MCFC versus other fuel cells-Characteristics, technologies and prospects," *Journal of Power Sources*, vol. 160, no. 2, pp. 858–862, 2006.

[6] B. G. Pollet, "The use of ultrasound for the fabrication of fuel cell materials," *International Journal of Hydrogen Energy*, vol. 35, no. 21, pp. 11986–12004, 2010.

[7] E. A. Cho, U. S. Jeon, H. Y. Ha, S. A. Hong, and I. H. Oh, "Characteristics of composite bipolar plates for polymer electrolyte membrane fuel cells," *Journal of Power Sources*, vol. 125, no. 2, pp. 178–182, 2004.

[8] H. N. Yu, J. W. Lim, J. D. Suh, and D. G. Lee, "Axiomatic design of carbon composite bipolar Plates for PEMFC vehicles," *Journal of Power Sources*, vol. 196, pp. 9868–9875, 2011.

[9] R. Blunk, F. Zhong, and J. Owens, "Automotive composite fuel cell bipolar plates: hydrogen permeation concerns," *Journal of Power Sources*, vol. 159, no. 1, pp. 533–542, 2006.

[10] R. Blunk, M. H. Abd Elhamid, D. Lisi, and Y. Mikhail, "Polymeric composite bipolar plates for vehicle applications," *Journal of Power Sources*, vol. 156, no. 2, pp. 151–157, 2006.

[11] S. C. Tjong, "Structural and mechanical properties of polymer nanocomposites," *Materials Science and Engineering R*, vol. 53, no. 3-4, pp. 73–197, 2006.

[12] J. H. Du, J. Bai, and H. M. Cheng, "The present status and key problems of carbon nanotube based polymer composites," *EXPRESS Polymer Letters*, vol. 1, pp. 253–273, 2007.

[13] D. C. Montgomery, *Design and Analysis of Experiments*, Wiley, Hoboken, NJ, USA, 5th edition, 2001.

[14] E. T. Thostenson and T. W. Chou, "On the elastic properties of carbon nanotube-based composites: modelling and characterization," *Journal of Physics D*, vol. 36, no. 5, pp. 573–582, 2003.

[15] P. K. Mallick, *Fiber-Reinforced Composites*, CRC Press, Boca Raton, Fla, USA, 3rd edition, 2008.

[16] G. Pinto and A. K. Maaroufi, "Nonlinear electrical conductivity of tin-filled urea-formaldehyde-cellulose composites," *Polymer Composites*, vol. 26, no. 3, pp. 401–406, 2005.

[17] G. Pinto, A. K. Maaroufi, R. Benavente, and J. M. Pereña, "Electrical conductivity of urea-formaldehyde-cellulose composites loaded with copper," *Polymer Composites*, vol. 32, no. 2, pp. 193–198, 2011.

[18] H. Im, S. Yun, and J. Kim, "Electro conductivities of well-dispersed PMMA-g-MWNTs/6FDA-based polyimide composites: effect of chemical structure," *Polymer Composites*, vol. 32, no. 3, pp. 368–377, 2011.

[19] Q. Zhang, H. Xiong, W. Yan, D. Chen, and M. Zhu, "Electrical conductivity and rheological behavior of multiphase polymer composites containing conducting carbon black," *Polymer Engineering and Science*, vol. 48, no. 11, pp. 2090–2097, 2008.

[20] E. P. Mamunya, V. V. Davidenko, and E. V. Lebedev, "Percolation conductivity of polymer composites filled with dispersed conductive filler," *Polymer Composites*, vol. 16, pp. 319–324, 1995.

[21] M. O. Lisunova, Y. P. Mamunya, N. I. Lebovka, and A. V. Melezhyk, "Percolation behaviour of ultrahigh molecular weight polyethylene/multi-walled carbon nanotubes composites," *European Polymer Journal*, vol. 43, no. 3, pp. 949–958, 2007.

[22] S. Hänsch, R. Socher, D. Pospiech, B. Voit, K. Harre, and P. Pötschke, "Filler dispersion and electrical properties of polyamide 12/MWCNT-nanocomposites produced in reactive extrusion via anionic ring-opening polymerization," *Composites Science and Technology*, vol. 72, pp. 1671–1677, 2012.

[23] M. T. Müller, B. Krause, and P. Pötschke, "A successful approach to disperse MWCNTs in polyethylene by melt mixing using polyethylene glycol as additive," *Polymer*, vol. 53, pp. 3079–3083, 2012.

[24] R. Socher, B. Krause, M. T. Müller, R. Boldt, and P. Pötschke, "The influence of matrix viscosity on MWCNT dispersion and electrical properties in different thermoplastic nanocomposites," *Polymer*, vol. 53, pp. 495–504, 2012.

[25] A. Allaoui, S. Bai, H. M. Cheng, and J. B. Bai, "Mechanical and electrical properties of a MWNT/epoxy composite," *Composites Science and Technology*, vol. 62, no. 15, pp. 1993–1998, 2002.

[26] M. B. Heaney, "Measurement and interpretation of nonuniversal critical exponents in disordered conductor-insulator composites," *Physical Review B*, vol. 52, no. 17, pp. 12477–12480, 1995.

[27] Y. P. Mamunya, Y. V. Muzychenko, P. Pissis, E. V. Lebedev, and M. I. Shut, "Processing, structure, and electrical properties of metal-filled polymers," *Journal of Macromolecular Science—Physics*, vol. 40, no. 3-4, pp. 591–602, 2001.

[28] A. Celzard, G. Furdin, J. F. Marêché, E. McRae, M. Dufort, and C. Deleuze, "Anisotropic percolation in an epoxy—graphite disc composite," *Solid State Communications*, vol. 92, no. 5, pp. 377–383, 1994.